

Design and Experimental Study of a Pneumatic Bionic Stingray Undulatory Soft Robot

Songzi Guo, Jinhua Zhang, Yuhan Yang, Haiyan Cheng and Jun Hong

Key Laboratory of Education, Ministry for Modern Design and Rotor-Bearing System, Xi'an Jiaotong University, Xi'an 710049, China

Keywords: Bio-Mimic Design, Flexible Actuation.

Abstract: Underwater organisms have always been providing inspiration for the design and development of novel underwater propulsion and bionic robots. At present, stingray has been taken as a bionic object due to its stable motion and robust mobility. In this study, a stingray propelled by flexible pectoral fins was taken as a bionic object. Based on this, a new idea for the design of high-performance bionic underwater propulsor was proposed. An analysis was conducted regarding the design, fabrication and experiments of the bionic stingray wave propulsion soft robot based on pneumatic drive. As revealed by the experiments of propulsion performance, the influencing factors for average propulsion include varying frequencies, fin stiffness and the gaps between substrate and the fins. This is expected to provide guidance on our design of a stingray robot in respect of efficient mobility.

1 INTRODUCTION

With the deepening of research on fish, researchers have found out that fish is adaptive to different living environments. By means of distinctive swimming gaits, fish is capable of high-speed cruise and agile maneuverability (Webb et al., 1994). Among various fishes, the stingray shown in Figure.1 is considered to be an outstanding swimmer especially when they swim in close proximity of the substrate (B. Liu and Z. Guo, 2018). Besides, it shows such obvious advantages high propulsion efficiency, excellent steering maneuverability and swimming stability, which makes it attract increasing attention from many researchers. According to the observation of a pectoral during swimming, there are multiple propulsive waves created by their pectoral fin, which are termed undulatory-swimmer. At present, there have been plenty of studies conducted on the motion mechanism of rays (Wu et al., 1961) as well as the swimming performance (Rosenberger et al., 1999 and 2001). These studies have provided us with a significant inspiration in the design of bionic robots (e.g. undulatory soft robotic (Urai, R. Sawada and N. Hiasa, 2015; Jusufi et al., 2017; S. N. Toda Y et al., 2006; Moored et al., 2011) and oscillatory soft robotic (Moored, K. W. and Dewey, P. A, 2011; Chen et al., 2012; Chew et al., 2015).

Based on the morphological properties of rays with independent actuators, a mimic soft batoid robot was developed in the previous work of Urai and Sawada (Urai, R. Sawada and N. Hiasa, 2015). Such specialized flexible structure makes the mimic soft batoid robot adaptive to a wide range of different applications and complex environmental conditions. Besides, it was indicated in their work that the fin stiffness causes swimming performance to vary significantly. Accordingly, an appropriate design of the fin stiffness is required to enhance swimming performance. Using ionic polymer-metal composite (IPMC), Chen et al (Chen et al., 2012) developed a manta ray robot to fabricate artificial muscles for the simulation of swimming behavior exhibited by a manta ray. According to their experimental results, this robot is capable to swim at 0.74 cm/s with a consumption of less than 2.5 W.

In this study, a finalized prototype of a bio-inspired stingray robot was developed through the combination of biomimetic functions and morphological properties. Furthermore, in order to enhance its swimming performance, the fin-to-wing extension stiffness for fins based on a jamming method was designed. However, this jamming method shows some difference compared with real rays, it is still a more effective approach to adjusting the stiffness of a pectoral fin than to replacing fin rays on it. Then, an experiment platform was constructed

to study the propulsion performance of the prototype. As revealed by the experimental results of propulsion performance, there is a significant improvement of average propulsion with the rising frequencies under 1Hz. Besides, it is determined by fin stiffness and shows an increase of negative pressure in jamming chamber. Then, an investigation was conducted into the impact of the bionic stingray robot on the propulsion performance when swimming took place at different heights from a substrate. The experimental results demonstrated that swimming performance can be enhanced by swimming close to the substrate at proper heights. The contributions of this study are threefold. Firstly, the novel pneumatic stingray robot was developed. Secondly, a jamming method was proposed for active variable stiffness to enhance propulsion force. Thirdly and lastly, the ground effect of the stingray robot on propulsion performance was verified.

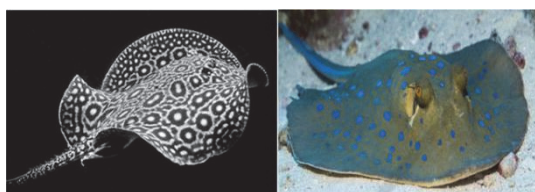


Figure 1: Biological stingrays.

2 FROM BIOLOGICAL FISH TO ROBOTIC FISH

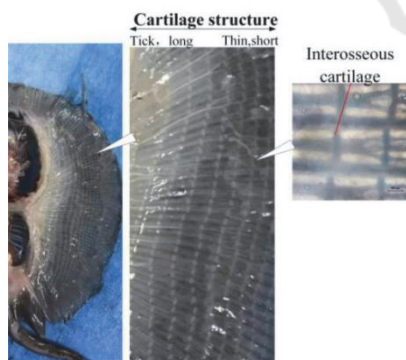


Figure 2: The skeletal structure of a stingray.

A rajiform swimmer, bluespotted stingray, is taken as an biomimetic subject, which is because its swimming model embodies a fine balance reached between speed and maneuverability, thus facilitating the design of a next-generation underwater vehicle. On this basis, a scheme was proposed to develop a stingray robot by combining both morphological and

kinematic properties of the stingray. In order to illustrate their excellent swimming performance, a series of vivisection experiments were conducted on a bluespotted stingray. The musculoskeletal structure of the subject is shown in Figure. 2, which reveals that the radial cartilage skeleton is embedded in a circular pectoral fin, which is covered with planate muscles. This sort of radially musculoskeletal structure is considered favorable for the agile and flexible motion of the pectoral fin by the successive stimulation of planate muscles. Moreover, an observation was made of the interosseous cartilage structure along the chordwise direction, and such a conjunction structure between two radial cartilages increases the chordwise stiffness in the pectoral fin required for the actual transmission of traveling wave in the chordwise direction (Fiazza et al., 2010). On the other hand, the compliant tissue, particularly on the pectoral fin, allows for bending to a greater extent, which prompts the shift of our focus to the enhancement of material properties that make the stingray robot closer to the object of simulation, for example, flexibility and malleability.

Based on the biological observations of anatomical structure, it is deemed necessary to simulate the existence of a radially musculoskeletal structure and the compliance of the pectoral fin, which is achieved through the symmetrical and radial deployment of twelve soft pneumatic actuators on the pectoral fin. In addition, it is essential to choose an appropriate material to approach the simulation object. Therefore, a variety of hyperelastic silicone rubber (ELASTOSIL, M4601) was adopted to fabricate the bionic actuators due to its excellent flexibility and malleability. The actuator is designed to combine an actuating chamber with two antagonist chambers and a jamming chamber as shown in Figure.3.a, in which the pressures are controlled separately. Constrained by winding fiber, this actuating chamber is covered with an external jacket made of the same material. A jamming chamber capable to adjust stiffness distribution on the pectoral fin is attached at the tip of an actuating chamber by wacker E41 as adhesive. As packed with plastic granules 2mm in diameter (Figure.3.d), While being depressurized, the cavity makes uncompacted granule compressed tightly and presents different stiffness. This method is effective in enhancing swimming performance, which will be verified in the following experiments. The total length of the actuator is 105mm, while the actuating part and jamming part are 70mm and 35mm in length, respectively, as shown in Figure.3.b. The fabrication process of the actuating chamber is illustrated in Figure.3 c. With the M4601

polymer poured into a 3D printed bladder mold and cured, the preliminary bladder is achieved after the first-time demolding. Then, it is wound with fiber to withstand the deformation caused in radial direction, as a result of which curvature can be generated when the pressure is increased in one chamber. Afterwards, the bladder is covered with jacket layer. After the second-time demolding and attachment of the jamming chamber at the tip of the fin ray, the fabrication of the entire actuator is completed.

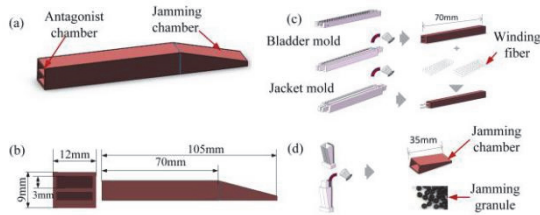


Figure 3: The design of the actuating fin ray with two degrees of freedom, (a) an isometric view, (b) a side view, consisting of actuating chamber and jamming chamber. (c) The fabrication process of the actuating fin rays involves bladder molding and jacket molding. (d) The fabrication process of the the jamming chamber. When depressurized, it makes uncompacted granules compressed tightly and exhibits varying stiffness.

When all of the twelve flexible fin rays are obtained, they are adhered to a disc-like transparent silicon rubber plate with a 0.5mm thickness.

3 EXPERIMENTS AND RESULTS

3.1 The Establishment of the Experimental Platform

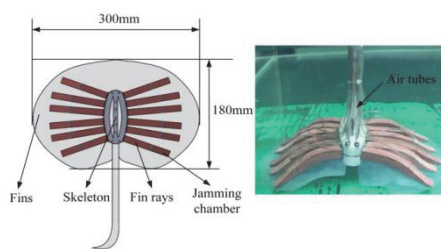


Figure 4: The developed prototype of the ray-like soft robot.

The bio-inspired stingray robot and its specifications are shown in Figure.4. The pectoral fin consists of dozen of the bionic fin rays deployed radially around the flexible disc-like plate. Besides, it is fixed on a skeleton made out of photosensitive resin. In order to provide and regulate the driving pressure, an air tube (SMC, 2mm) is supposed to be connected to each of

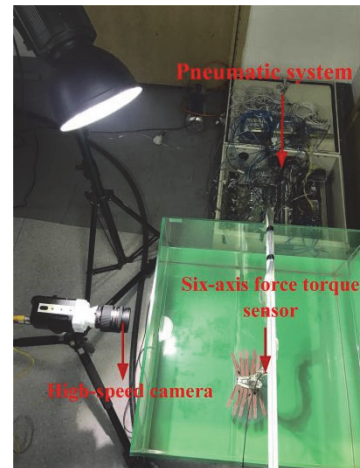


Figure 5: An experiment system to test the swimming performance.

the antagonist chambers actuated separately by a pneumatic system, as shown in Figure.5. The pneumatic system primarily consists of an air compressor module capable of supplying compressed air to the actuators and a digital output module achieved by a PLC module (OMRON, CJ1W-DA08V, CJ1W-OC21), which is capable to regulate the states of solenoid valves and proportional valves, respectively. The pneumatic system is placed above the water. Air tubes are applied to connect the pneumatic system to the bionic stingray robot. Considering that one of the most representative properties of bio-inspired robots, flexibility, can be affected when they are combined with rigid electronic components, a simplified prototype with open loop control was developed without any type of electrical components fitted on the bionic stingray robot. This open loop control is capable of regulating the undulatory attitudes, frequencies and the stiffness of the fin rays. More specifically, it can regulate the compressed air generated by the air compressor module and make adjustment to the pressure in the two antagonist chambers when the solenoid valves and proportional valves are successively exerted sinusoidal signals generated by the PLC module to control its states. Then, the bionic stingray robot can perform distinct undulatory gaits. The deformation caused to the pectoral fins of the bionic stingray robot is illustrated in Figure. 6.a, which shows that it is driven by a pressure regulated by the PLC module. The maximum pressure in the actuating chambers is 0.08Mpa, and the actuating frequency is 0.5Hz. As shown in Figure. 6.b, the bionic stingray robot is snapped while performing an undulatory gait.

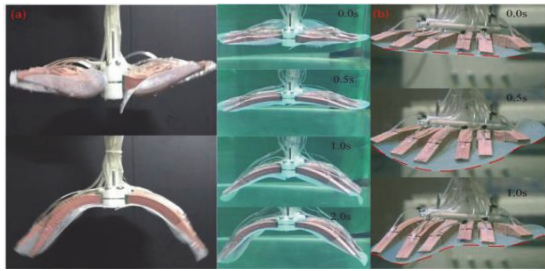


Figure 6: The deformation on the pectoral fins of the stingray robot.

3.2 Effects of Frequencies on Propulsion Performance

In order to explore the relationship between the frequency and propulsion, the stingray robot was placed in a water tank which is 1.5m long, 1m wide and 0.5m deep, the locomotion of which was restricted to one degree of freedom for a forward translation with a steel bar. The swimming behavior on propulsion was observed by periodically driving the fin rays in phase at varying frequencies. The average propulsion was obtained by measuring the propulsion within one period. In the experiments, a 6-axis force torque sensor (ATI-Nano17) was employed to record the forces generated. More specifically, the undulatory amplitude was significantly down-regulated to actuate frequencies over 2.5Hz due to the limitation on the response time of the pneumatic system. Thus, the maximum driving frequency was restricted to under 2Hz. It was found out that a decent undulatory amplitude appeared on the fin under the driving pressure $P = 0.05\text{Mpa}$. Therefore, the experiments were conducted under the actuating pressure of 0.05MPa.

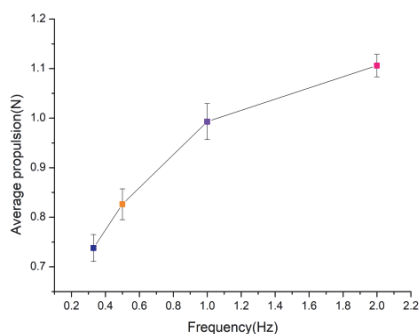


Figure 7: The propulsion performance for four different frequencies $f = 0.33, 0.50, 1.00, 2.00$ Hz.

The experimental results indicate the relationship between average propulsion and the actuating frequencies, as shown in Figure.7. The average propulsion is affected by the changes in frequency.

On the one thing, the average propulsion is improved with the rise of frequency and one maximum average propulsion can reach 1.1N. In the meantime, the driving frequency and pressure are 2.00Hz and 0.05MPa, respectively. When the actuating frequency exceeds 1Hz, nevertheless, this upward trend begins to slow down. On the other hand, a higher level of frequency requires the consumption of more energy. Thus, it is necessary for both propulsion and energy consumption to be considered carefully for meeting different requirements.

3.3 Effects of Fin Stiffness on Propulsion Performance

Given that fishes can create a greater propulsion force to change the stiffness of their fins and have interaction with the surrounding fluid in a flexible way (Fiazza et al., 2010), our stingray robot with a jamming chamber at the tip of the fin ray is optimized to enhance the propulsion performance while allowing it to get adaptive to various hydrodynamic circumstances. The experiments were performed to better understand how the propulsion force varies for the fins to achieve different stiffness after being depressurized to different pressures. The propulsion forces were measured during the one period $T=3\text{s}$ with jamming chamber for three different pressures ($P_j = 0\text{kPa}, -30\text{kPa}, -60\text{kPa}$), and the twelve fin rays were driven under pressure $P = 0.05\text{Mpa}$.

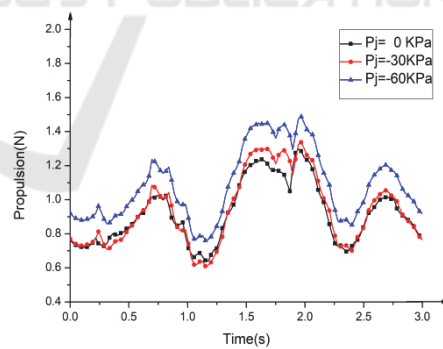


Figure 8: Propulsion of the stingray robot with three different fin stiffness regulated by negative pressure in the jamming chamber (P_j stands for the negative pressure in jamming chamber).

The difference of propulsion forces at varying negative pressure is shown in Figure.8, in which the propulsion forces of three different negative pressures are plotted. According to the experimental results, the propulsion force is maximized when the jamming chambers are depressurized to -60kPa. By contrast, the propulsion force is minimized under the pressure

$P=0\text{kPa}$. Additionally, each side of the fin rays is divided into three pairs driven by the actuating signal in different phases. Since the motion of fins is based on three pairs of fin rays, three different propulsion peaks can be observed in Figure.9 and the largest propulsion force is indicated by the middle peak, which suggests that the middle pair plays a crucial role in this stipulated pattern of motion. Moreover, it is worth noting that the maximum undulatory amplitude of the stingray robot is reduced as negative pressure rises (0kPa through -60kPa) in jamming chamber. In comparison, the driving pressure and frequency remain unchanged. Therefore, the stiffness of the fins is required to meet the various requirements.

3.4 The Ground Effect on Swimming Performance

It is noteworthy that when fishes swim near the substrate, its generation of propulsion is subject to a significant impact from the distance between the fins and the substrate (B. Liu and Z. Guo, 2018). In the experiments conducted in this study, the propulsion performance of the fins was investigated with three different gaps ($d=10\text{cm}$, 20cm , 30cm) between the fins and ground. Moreover, each of the experiment was conducted under the same driving pressure $P=0.05\text{MPa}$ and frequency $f=0.5\text{Hz}$.

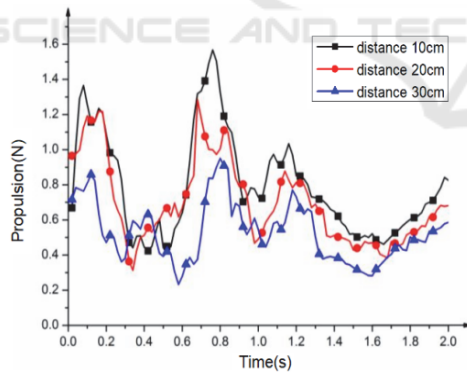


Figure 9: Propulsion of the stingray robot with different distances between the substrate and the bionic pectoral fin.

The result is shown in Figure.9, which reveals that the maximum value can reach 1.6 N when the gap is 10cm . In this case, its trajectory of propulsion force shows a slight difference with gap $d=20\text{cm}$ and gap $d=30\text{cm}$, the instantaneous maximum of which can reach 1.28 N and 0.92 N , respectively. In addition, near-ground swimming can generate three different propulsion peaks in one period, which is associated with the motion of fins. The propulsion peaks will be

observed when the fin rays close to the ground, suggesting that the stingray robot can achieve a superior propulsion performance when it swims at a proper height (10cm), which is conducive to enhancing the efficiency of underwater propulsor.

4 CONCLUSION

In this study, a prototype of stingray robot based on the combination of biological functions and morphological properties was proposed to make the stingray robot capable of achieving ray-like flexible locomotion through a pneumatic system. The biological functions including rapid responding and agile motion are estimated by propulsion forces and the average propulsion can reach 1.1N at maximum. In comparison, the driving frequency and pressure are 2.00Hz and 0.05MPa , respectively. Moreover, the propulsion performance of the stingray robot can be enhanced by adjusting the stiffness of their fins and having interaction with the surrounding fluid in a flexible way as achieved by jamming method and flexible biomimetic material. The inherent advantages of the pneumatic actuator, especially in weight and deformation, provide a new idea for the design of underwater vehicles fit for complex working environments. Moreover, the constant change made to the stiffness on bionic fin rays using the depressurized jamming method allows bionic underwater vehicles to adjust stiffness distribution. According to the results of ground effect on swimming performance, a proper operational depth is also beneficial to improve the propulsion performance of ray-like underwater vehicles.

In the future, a further study in this regard should focus on two aspects as follows. Firstly, judging on a serial of frames recorded by the high-speed camera, the undulatory amplitude of the pectoral fin is partially limited by the disc-like base that radially carries dozen of the fin rays. In addition, this constraint placed on the fin rays results in a slightly lateral distortion and vibration when these fin rays are actuated over a certain pressure to perform undulatory gaits. It is considered as a disadvantage, especially when loop-controls are introduced into the robotic system. Therefore, one of the improvement that can be made in the further research is to chose a more resilient material to minimize this potential interference. Secondly, the introduction of loop-controls to the robotic system is effective in improving the swimming performance of the bionic stingray robot. As a support for gathering the information about motion, a control method based on

nonlinear error feedback controller will be introduced and a flexible sensor will be fitted on our next-generation prototype.

Manta Ray. IEEE International Conference on Robotics & Biomimetics. IEEE.
Fiazza, C. ,Salumae, T. , Listak, M. , Kulikovskis, G. , & Kruusmaa, M. (2010). Biomimetic mechanical design for soft-bodied underwater vehicles. Oceans IEEE-SYDNEY. IEEE.

ACKNOWLEDGEMENTS

This research was financially supported by the National Nature Science Foundation of China (No. 91748123).

REFERENCES

- Webb, P. (1994). The biology of fish swimming. In L. Maddock, Q. Bone, & J. Rayner (Eds.), *The Mechanics and Physiology of Animal Swimming* (pp. 45-62). Cambridge: Cambridge University Press.
- Liu and Z. Guo, (2018). Ground effect on the hydrodynamic performance of a flexible hinge-connected fin. *IEEE/ASME Int. Conf. Adv. Intell. Mechatronics, AIM*, vol. 2018-July, pp. 881–886, 2018.
- Wu, T. . (1961). Swimming of waving plate. *journal of fluid mechanics*, 100.
- Rosenberger, L. J., & Westneat, M. W. (1999). Functional morphology of undulatory pectoral fin locomotion in the stingray *taeniura lymma* (chondrichthyes: dasyatidae).
- Rosenberger, L. J., (2001). Pectoral fin locomotion in batoid fishes: undulation versus oscillation. *Journal of Experimental Biology*, 204(Pt 2), 379-394.K.
- Urai, R. Sawada, N. Hiasa, M. Yokota, and F. DallaLibera. (2015). Design and control of a ray-mimicking soft robot based on morphological features for adaptive deformation. *Artificial Life & Robotics*, 20(3), 237-243.
- Jusufi, A., Vogt, D. M., Wood, R. J., & Lauder, G. V.. (2017). Undulatory swimming performance and body stiffness modulation in a soft robotic fish-inspired physical model. *soft robot*, 202-210.
- S. N. Toda Y, Sanada Y, and Danno M. .(2006). The motion of a fish-like under-water vehicle with two undulating side fins. *Proceedings of the 3rd International Symposium on Aero Aqua Bio-mechanisms*.
- Moored, K. W. , Fish, F. E. , & Kemp, T. H. . (2011). Batoid fishes: inspiration for the next generation of underwater robots. *Marine Technology Society Journal*, 45(4).
- Moored, K. W. , Dewey, P. A. , Leftwich, M. C. , Bart-Smith, H. , & Smits, A. J. . (2011). Bioinspired propulsion mechanisms based on manta ray locomotion. *Marine Technology Society journal*, 45(4), p.110-118.
- Chen, Z. , & Bart-Smith, H. . (2012). Bio-inspired robotic manta ray powered by ionic polymer-metal composite artificial muscles. *International Journal of Smart & Nano Materials*, 3(4), p.296-308.
- Chew, C. M. , Lim, Q. Y. , & Yeo, K. S. . (2015). Development of propulsion mechanism for Robot